Am J Nucl Med Mol Imaging 2012;2(4):483-498
www.ajnmmi.us /ISSN:2160-8407/ajnmmi1208002

Original Article

Efficient multicistronic co-expression of hNIS and hTPO in prostate cancer cells for nonthyroidal tumor radioiodine therapy

Guoquan Li[1,2,*], Lei Xiang[3,*], Weidong Yang[1], Zhe Wang[1], Jing Wang[1], Kai Chen[2]

[1]Department of Nuclear Medicine, Xijing Hospital, The Fourth Military Medical University, Xi'an, Shaanxi, China, 710032; [2]Molecular Imaging Center, Department of Radiology, Keck School of Medicine, University of Southern California, CA 90033, USA; [3]Department of Pediatrics, Shaanxi Maternal and Child Care Service Center, Xi'an, Shaanxi, China, 710003. [*]These authors contributed equally to this work.

Received August 6, 2012; Accepted August 24, 2012; Epub October 15, 2012; Published October 30, 2012

Abstract: Radioiodine therapy has proven to be a safe and effective approach in the treatment of differentiated thyroid cancer. Similar treatment strategies have been exploited in nonthyroidal malignancies by transfecting hNIS gene into tumor cells or xenografts. However, rapid radioiodine efflux is often observed after radioiodine uptake, limiting the overall antitumor effects. In this study, we aimed at constructing multicistronic co-expression of hNIS and hTPO genes in tumor cells to enhance the radioiodine uptake and prolong the radioiodine retention. Driven by the cytomegalovirus promoter, hNIS and hTPO were simultaneously inserted into the expression cassette of adenoviral vector. An Ad5 viral vector (Ad-CMV-hTPO-T2A-hNIS) was assembled as a gene therapy vehicle by Gateway technology and 2A method. The co-expression of hNIS and hTPO genes was confirmed by a double-label immunofluorescence assay. The radioiodine (^{125}I) uptake and efflux effects induced by co-expression of hNIS and hTPO genes were determined in transfected and non-transfected PC-3 cells. Significantly higher uptake (6.58 ± 0.56 fold, at 1 h post-incubation) and prolonged retention (5.47 ± 0.36 fold, at 1 h of cell efflux) of radioiodine (^{125}I) were observed in hNIS and hTPO co-expressed PC-3 cells as compared to non-transfected PC-3 cells. We concluded that the new virus vector displayed favorable radioiodine uptake and retention properties in hNIS-hTPO transfected PC-3 cells. Our study will provide valuable information on improving the efficacy of hNIS-hTPO co-mediated radioiodine gene therapy.

Keywords: Gene therapy, prostate cance, hNIS, hTPO, gateway cloning system

Introduction

Human sodium/iodide symporter (hNIS) is a transmembrane glycoprotein which transports two sodium cations for each iodide anion into the cell. hNIS is responsible for mediating iodide uptake and is consequently essential for thyroid hormone synthesis in thyroid cells [1, 2]. The enhancement of hNIS has been found in thyroid cancer cells, leading to an approach of radioiodine therapy with improved efficacy [3, 4]. Human thyroperoxidase (hTPO) is an enzyme expressed mainly in the thyroid that catalyzes iodination of tyrosine residues of thyroglobulin and promotes iodide retention within thyroid cells [5]. Expression of both hNIS and hTPO induces rapid radioiodine accumulation and organification in thyroid cancer cells, resulting in improved DNA damage and tumor cell death [6].

In the past decade, hNIS transgene strategy has been exploited in nonthyroidal tumors such as lung cancer, liver cancer, colon cancer, and prostate cancer [7-10]. However, because of the deficiency of iodine organification, the iodide usually undergoes rapid efflux by an active process [1-4] from hNIS gene transfected cells, which reduces the antitumor efficacy [11]. Subsequently, an advanced strategy of hTPO/hNIS co-transfection was proposed to achieve increased radioiodine uptake and prolonged radioiodine retention [12].

In this study, we aimed at maximizing the advantages of i) hNIS function for enhancement of

iodine uptake, and ii) organification function of hTPO for iodine retention by a means of constructing multicistronic co-expression of hNIS and hTPO genes in tumor cells. We constructed an Ad5 viral vector (Ad-CMV-hTPO-T2A-hNIS) as a gene therapy vehicle through simultaneously inserting hNIS and hTPO into the expression cassette of adenoviral vector. T2A (Thosea asigna virus 2A sequence) was introduced as a linker between hTPO and hNIS gene to allow automatic self-cleavage of polyprotein. We hypothesized that this multicistronic viral vector would enable more efficient radioiodine uptake and prolonged radioiodine retention in transfected cancer cells. We anticipated that the outcome of our research would provide a promising approach for the treatment of regionally advanced cancers.

Materials and methods

Construction of pAV.Ex1d-CMV>hNIS and pAV.Ex1d-CMV>hTPO/T2A/hNIS by gateway technology

The general strategies employed for construction and characterization of pAV.Ex1d-CMV>hNIS and pAV. Ex1d-CMV>hTPO/T2A/hNIS are summarized in **Figures 1** and **2**.

Isolation and characterization of hNIS and hTPO cDNA

The full-length hNIS cDNA was removed from the hNIS gene (kindly provided by Dr. Biao Li at the Shanghai Jiaotong Medical University) by restriction digestion. The sequence of obtained hNIS cDNA was confirmed by sequencing analysis as compared to the hNIS gene in the GenBank (ID of hNIS: HH762189.1). In addition, the obtained hNIS cDNA was inserted into eukaryotic expression vector pcDNA followed by digestion using restriction enzyme EcoRI/HindIII. The digested hNIS cDNA was then analyzed by AGE (agarose gel electrophoresis) to confirm its size.

The hTPO cDNA was cut out from the pDNR-LIB-hTPO-M plasmid (Changsha Yingrun Biotechnology Co., China) mutated at the point of the 208th base from G to C as compared to the hTPO gene in the GenBank (ID of hTPO: BC095448.1). Similar to the characterization of hNIS cDNA, the mutated hTPO cDNA was confirmed by sequencing analysis and AGE.

PCR amplification of attB1/hNIS/attB2, attB1/hTPO/attB2, and attB1/hTPO/T2A/hNIS/attB2

PCR amplification of attB1/hNIS/attB2 (or attB1/hTPO/attB2): PCR was performed in 50 μL of assay solution containing 0.5 μL of Primer STAR™ HS DNA Polymerase (Takara Bio, Inc.), 10 μL of 5 × Primer STAR™ buffer (Mg^{2+} Plus), 4 μL of dNTP mixture (10 μM), primary forward and reverse primers (primer-F: attB1-Kozak-hNIS, sequence listed in **Table 1**; primer-R: attB2-hNIS, sequence listed in **Table 1**, 1 μL of each primer (10 μM)), and 1 μL of hNIS (or hTPO) genomic cDNA. The mixture was heated at 98°C for 3 min followed by additional 30 PCR cycles (98°C for 10 s, 60°C for 10 s, and 72°C for 2 min per circle). The amplified attB1/hNIS/attB2 (attB1/hTPO/attB2) fragment was incubated at 72°C for 5 min to form the final PCR products, which were then purified by QIAquick Gel Extraction Kit (QIAGEN) and stored at -20°C until use.

PCR amplification of attB1/hTPO/T2A/hNIS/attB2: The basic PCR procedure was performed as described above, except for using different primers. The 5'T2A-3'hTPO and attB1-Kozak-hTPO primers were used to generate attB1-hTPO-T2A, while the 3'T2A-5'hNIS and attB2-hNIS primers were applied to yield attB2-hNIS-T2A. The obtained attB1-hTPO-T2A and attB2-hNIS-T2A (as genomic DNAs) then reacted with attB2-hNIS and attB1-Kozak-hTOP (as primers) to form the attB1/hTPO/T2A/hNIS/attB2 products. Afterwards, Fusion primer F and R were used to amplify the attB1/hTPO/T2A/hNIS/attB2 to provide the final products, which were then purified by QIAquick Gel Extraction Kit (QIAGEN) and stored at -20°C until use.

Recombination of attB × attP – construction of pDown-hNIS, pDown-hTPO, and pDown-hTPO/T2A/hNIS

Construction of pDown-hNIS (or pDown-hTPO): The previously amplified attB1/hNIS/attB2 (or attB1/hTPO/attB2) was inserted into the vector pDONR™/221 (Life Technologies, Inc.) by using the BP Clonase™ II Enzyme Mix (Life Technologies, Inc.). Briefly, in a 96-well plate, samples containing 200 ng of attB1/hNIS/attB2 (or attB1/hTPO/attB2), 1 μL of BP Clonase™ II Enzyme Mix, 100 ng of pDONR™

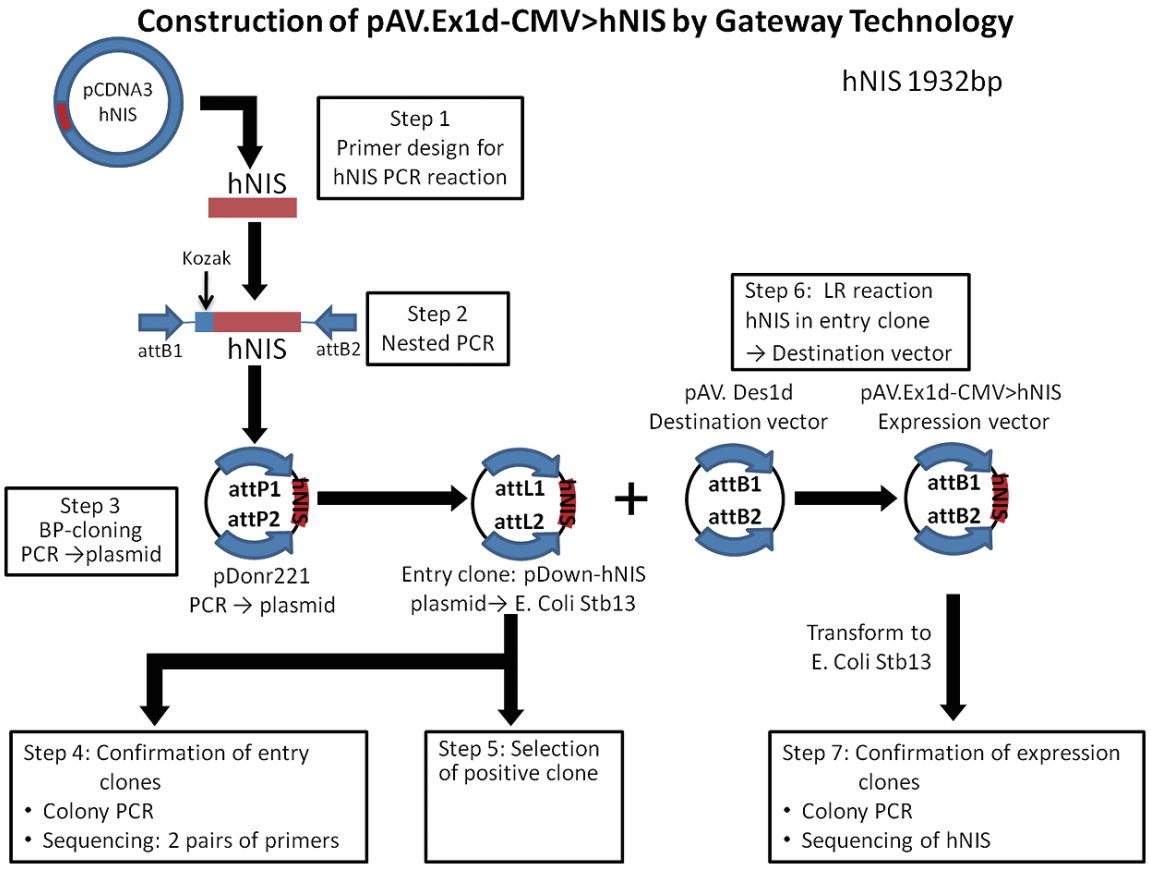

Figure 1. Schematic representation of the pAV.Ex1d-CMV>hNIS construction. The PCR products after hNIS amplification were used for a BP reaction, followed by bacterial transformation and sequencing verification. After the selection of positive clones, the pAV.Ex1d-CMV>hNIS gene was generated and validated by functional analysis.

Table 1. Primers used in PCR amplification of attB1/hNIS/attB2, attB1/hTPO/attB2, and attB1/hTPO/T2A/hNIS/attB2.

Primers		Oligo sequence (from 5' to 3')
hNIS	attB1-Kozak-NIS	GGGGACAAGTTTGTACAAAAAAGCAGGCTGCCACC ATGGAGGCCGTGGAGACC
	attB2-hNIS	GGGGACCACTTTGTACAAGAAAGCTGGGTTCAGAGGTTTGTCTCCTGCTG
hTPO	attB1-Kozak-hTPO	GGGGACAAGTTTGTACAAAAAAGCAGGCTGCCACCAGAGGAATCCTTTCTCCAGCTCAGCTTCTGT
	attB2-hTPO	GGGGACCACTTTGTACAAGAAAGCTGGGTACAGAAGCTGAGCTGGAGAAAGGATTCCTCT
hTPO/T2A/hNIS	attB1-Kozak-hTPO	GGGGACAAGTTTGTACAAAAAAGCAGGCTGCCACCATGAGAGCGCTGGCTGTGC
	5'T2A-3'hTPO	GTCCCCGCATGTTAGAAGACTTCCCCTGCCCTCTCCGGAGCCGAGGGCTCTCGGCAGCC
	3'T2A-5'hNIS	GTCTTCTAACATGCGGGGAC GTGGAGGAAAATCCCGGCCCCATGGAGGCCGTGGAGACC
	Fusion primerF	GGGGACAAGTTTGTACAAAAAAGCAGGCTGCCACCATG
	Fusion primerR	GGGGACCACTTTGTACAAGAAAGCTGGGTTCAGAGGTTTGTC

/221 plasmid, and 1–5 μL of TE buffer (pH 8.0) were incubated at 25°C for 3 h. Proteinase K (1 μg, Life Technologies, Inc.) was then added into the samples and incubated at 37°C for 30 min. The pDown-hNIS (or pDown-hTPO) products from the BP reaction (recombination of attB × attP) were directly used for bacterial transformation.

Construction of pDown-hTPO/T2A/hNIS: The procedure was performed similarly to the construction of pDown-hNIS as described above,

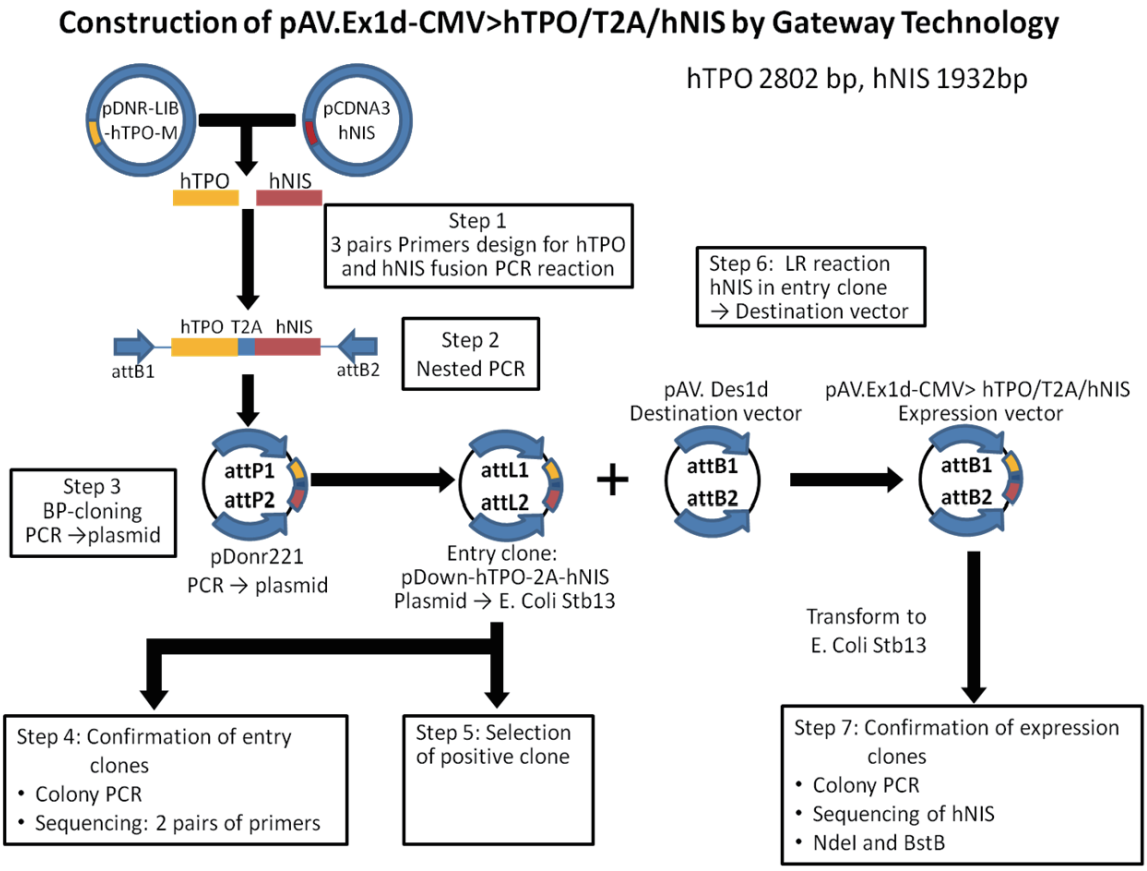

Figure 2. Schematic representation of the pAV.Ex1d-CMV>hTPO/T2A/hNIS construction. The PCR products after hNISs and hTPOs amplification were used in the first step for a BP reaction, followed by bacterial transformation and sequencing verification. After the selection of positive clones, the pAV.Ex1d-CMV>hTPO/T2A/hNIS gene was generated and validated by functional analysis.

except for using attB1/hTPO/T2A/hNIS/attB2. The pDown-hTPO/T2A/hNIS products from the BP reaction (recombination of attB × attP) were directly used for bacterial transformation.

Bacterial transformation

An aliquot (2 μL) from pDown-hNIS (or pDown-hTPO; or pDown-hTPO/T2A/hNIS) products was added into a vial containing One Shot® stb13™ Chemicallly Competent Cells *E. coli* (Life Technologies, Inc.) according to the manufacturer's protocol. The samples were incubated in ice for 30 min. After heating at 42°C for 90 s, the samples were incubated in ice for 2 min following by adding of 300 μL of SOC medium (Life Technologies, Inc.). The samples were then incubated at 37°C for 1 h. After incubation, 100 μL of hNIS (or hTPO; or hTPO/T2A/hNIS) was seeded in low salt Luria-Bertani (LB) solid medium (containing 50 μg/mL of kanamycin, Life Technologies, Inc.) and incubated overnight at 37°C to produce a single colony. The remainder of transformation reaction was added into 150 μL of low-salt LB liquid medium (containing 50 μg/mL of kanamycin, Life Technologies, Inc.). The bacterial was cultured at 37°C overnight and then stored at -80°C until use.

Colony PCR of hNIS and hTPO bacterial clones

A single colony from transformation reaction was analyzed by PCR to verify the correct size of the inserted hNIS or hTPO. The hNIS (or hTPO) PCR was performed in a vial containing 30 μL of sample with 1.5 U Taq DNA Polymerase (Thermo Fisher Scientific, Inc.), pDONR™/221-specific forward primer (pUpDo-flank-f; sequence is listed in **Table 2**) (10 μM) and reverse primer (pUpDo-flank-r; sequence is listed in **Table 2**) (10 μM), dNTP mix (0.2 mM), 10× BioTherm™ reaction buffer (5 μM, 1.2 μL). A

Table 2. Primers used in sequencing of pDown-hNIS, pDown-hTPO, and pDown-hTPO/T2A/hNIS.

pDown-hNIS		pDown-hTPO/T2A/hNIS	
pUpDo-flank-f	CGGCCAGTCTTAAGCTCGGG	pUpDo-flank-f	CGGCCAGTCTTAAGCTCGGG
W1F	GGTCGTGGTGATGCTAAGTG	W1F	TCTATGAGGACGGCTTCAGT
pUpDo-flank-r	AATACGACTCACTATAGGGGA	W2F	ACGCCAGATCCAAGGTGC
W1R	GGAACATTCCCAAGATGAAG	W3F	GCGCAGAGACACTGGAAGCC
pDown-hTPO		W4F	AGGCACATCCAGAGGAACTT
pUpDo-flank-f	CGGCCAGTCTTAAGCTCGGG	W5F	CACCAGCAGAGGCATGTACT
W1F	TCTATGAGGACGGCTTCAGT	W6F	GGATGGCCACTTCTTCCTTG
pUpDo-flank-r	AATACGACTCACTATAGGGGA	pUpDo-flank-r	AATACGACTCACTATAGGGGA
W1R	ATGAGAGCGCTGGCTGTGC		

total of 29 PCR cycles (94°C for 30 s, 60°C for 30 s, and 72°C for 2 min per cycle) was preceded by heating to 94°C for 3 min and followed by 1-min incubation at 72°C. The sizes of PCR products were determined by AGE and ethidium bromide staining. Positive entry clones with pDown-hNIS (or pDown-hTPO) were selected and added into 150 μL of low-salt LB liquid medium (containing 50 μg/mL of kanamycin, Life Technologies, Inc.) and incubated overnight at 37°C. The entire culture was subject to plasmid isolation.

Identification by enzyme digestion for plasmid pDown-hTPO/T2A/hNIS

For enzyme digestion of pDown-hTPO/T2A/hNIS, 1 μg of plasmid DNA (Life Technologies, Inc.) was added directly into a mixture containing 1 μL of EcoRV (10 U), 1 uL of XhoI (10 U), 2 μL of restriction buffer (10× buffer 3), 0.2 uL of BSA (10 mg/mL), and 13.8 uL of deionized water. The mixture was incubated at 37°C for 60 min. After digestion, the sample was mixed with gel loading buffer and applied to a gel for electrophoretic analysis.

DNA sequencing of pDown-hNIS, pDown-hTPO, and pDown-hTPO/T2A/hNIS

Sequencing of plasmid DNA was performed using a standard dideoxy sequencing approach [13, 14]. A sample (10 μL) containing 5μL of plasmid, 0.32 μM primers (pUpDo-flank-f, W1F, pUpDo-flank-r, and W1R; sequences are shown in **Table 2**), 2 μL of BigDye® Terminator v3.1 Ready Reaction Mix (Life Technologies, Inc.), and 1 μL 5× sequencing buffer was heated at 95°C for 5 min followed by 25 cycles of extension reactions (95°C for 10 s, 50°C for 5 s, and 60°C for 90 s per cycle). After precipitating with sodium acetate and absolute ethanol, the resulting DNA was sequenced with an ABI 3730 xl Genetic Analyzer Capillary Array (Life Technologies, Inc.).

Recombination of attL×attR – construction of pAV.Ex1d-CMV>hNIS, pAV.Ex1d-CMV>hTPO, and pAV.Ex1d-CMV>hTPO/T2A/hNIS

Entry vectors were set up in an LR reaction to recombine the gene of interest into pAV.Des1d destination vectors. Samples containing 10 fmol pDown-hNIS (or pDown-hTPO; or pDown-hTPO/T2A/hNIS), 1 μL of LR Clonase™ II Enzyme Mix (Life Technologies, Inc.), pAV.Des1d destination vector (20 fmol), and 1–5 μL of TE buffer (pH 8.0) were incubated at 25°C for 16 h. Proteinase K (1 ug, Life Technologies, Inc.) was then added into the samples and incubated at 37°C for 30 min. The pAV.Ex1d-CMV>hNIS (or pAV.Ex1d-CMV>hTPO; or pAV.Ex1d-CMV>hTPO/T2A/hNIS) products from the LR reaction (recombination of attL × attR) were directly used for bacterial transformation.

Colony PCRs of pAV.Ex1d-CMV>hNIS (or pAV.Ex1d-CMV>hTPO) were performed as described above by using vector-specific primers (F: GAACCCACTGCTTACTGGCTT; R: TCGAGACCGAGGAGAGGGT) to verify successful cloning. To confirm pAV.Ex1d-CMV>hTPO/T2A/hNIS, similar enzyme digestion procedure was performed as described above except for using restriction buffer (10× buffer 4), and NdeI and BstBI as enzymes.

Packaging, amplification, concentration, and titration of the recombinant adenoviral vector carrying hNIS, or hTPO, or hTPO-T2A-hNIS

The expression vector pAV.Ex1d-CMV>hNIS (or pAV.Ex1d-CMV>hTPO; or pAV.Ex1d-CMV>hTPO/

T2A/hNIS) was digested by enzyme PacI to generate linear adenoviral plasmid by QIAquick Gel Extraction Kit (QIAGEN, Inc.). The human embryonic kidney HEK293cells were seeded into a 6-well plate (2 × 10^5 cells/well) containing DMEM supplemented with 10% FBS, and cultured at 37°C for 18–24 h in a CO_2 incubator (5% CO_2) until cells grew to 80%~90% confluency. The HEK293 cells were then transfected with the linear adenoviral plasmid (containing 250 μL of Opti-MEM, 1 μg of plasmid DNA, and 3 μL of lipofectine in each well) at 37°C for 24 h. The HEK293 cells continued to be incubated with 10% FBS for 7 days until the formation of viral plaques, referred to cytopathic effects (CPE), was visible in most of the cells. Virus were collected by performing freezing (-80°C) and melting (37°C) of the cells for three rounds, followed by centrifuging (4°C) at 2000 g for 10 min. The supernatant was then sub-packaged and frozen at -80°C. The virus was named as P0.

The process of repeated freezing and melting was adopted for amplification of adenovirus in HEK293 cells to obtain desired virus amount. HEK293 cells were cultured as described above. When cells grew to 80%~90% confluency, 100 uL of P0 virus was added into each culture flask and incubated with 5% CO_2 at 37°C until the CPE was visible in most of the cells. The cells and supernatant were then collected after centrifuging at 200 g for 10 min. The deposit was resuspended. After three rounds of freezing (-80°C) and melting (37°C) followed by centrifuging at 2000g for 10 min, the supernatant was sub-packaged and frozen at -80°C. The virus was named as P1. $TCID_{50}$ (50% tissue culture infective dose) assay was carried out to titrate the adenovirus. The procedure was performed similarly to described previously [15]. Finally, the titration value for the virus was calculated according to the Kärber formula ($T = 10^{s+0.8}$ PFU/mL) [16].

Cell culture of human prostate cancer PC-3 cells

Human prostate cancer PC-3 cells were grown at 37°C under an atmosphere of 5% CO_2 in air as monolayer in 25 cm^2 tissue culture flasks containing 5.0 mL of DMEM-F12 medium supplemented with 10% fetal bovine serum (FBS), 100 U/mL penicillin/streptomycin solution, and 2 mM glutamine (Life Technologies, Inc.).

Adenovirus-mediated hNIS and hTPO gene transfer of PC-3 cells

PC-3 cells were seeded in a 24-well tissue culture plate at a concentration of 5 × 10^4 cells/well. When cells confluence reached to 60–80%, the cell monolayers were transfected with the Ad-CMV-hTPO, Ad-CMV-hNIS, and Ad-CMV-hTPO-2A-hNIS (Multiplicity of Infection (MOI) = 20). Medium was replaced by fresh culture medium after 16 h and virus-infected cells were maintained for additional 48 h until use. All adenoviral infections were carried out in triplicates.

Immunofluorescence staining of hNIS and hTPO co-expression in transfected PC-3 cells

PC-3 cells were seeded in a 24-well plate 24 h before the experiment to reach a density of 1×10^5 cells/well on the day of infection. Cells were transfected with recombinant Ad5 virus described above (Ad-CMV-hTPO; or Ad-CMV-hNIS; or Ad-CMV-hTPO-2A-hNIS). After 48 h, cells were washed twice with PBS, and fixed for 20 min in 4% ice-cold paraformaldehyde. The cells were then washed twice with PBS and permeabilized with 0.2% Triton X-100 (in PBS) for 10 min. After two additional wash with PBS, the fixed cells were blocked with 5% BSA in PBS for 1 h at room temperature. The cells were then incubated with hNIS and hTPO antibody (mouse monoclonal anti-hNIS, 1:100, Lab Vision Co.; rabbit monoclonal anti-hTPO, 1:100, Abcam, Inc.), followed by PBS wash three times. The cells were incubated with anti-mouse and anti-rabbit fluorescein-conjugated secondary antibody (with a dilution of 1:100 in PBS, Lab Vision Co.) at 37°C for 1 h. After washing with PBS three times, the cells were directly observed by a fluorescence microscope (Olympus CKX41, Japan). The non-transfected cells served as the control.

Radioiodine (^{125}I) uptake and efflux

Radioiodine (^{125}I) uptake was measured to assess the function of hNIS and hTPO co-expressions in PC-3 cells according to the procedure described previously [17]. ^{125}I was purchased from Chengdu Gaotong Isotope Co., China. After 16 h gene transfection and additional 48 h maintenance, PC-3 cells were washed twice with 0.5 mL of HBSS buffer (supplemented with 10 uM sodium iodide and buff-

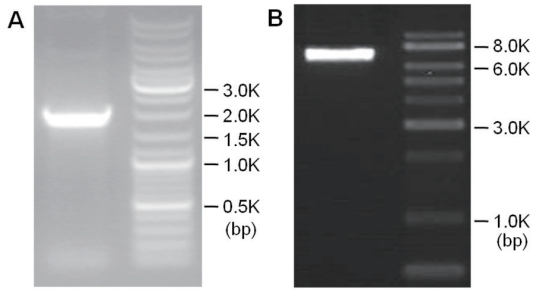

Figure 3. Characterization of hNIS and hTPO cDNA genes. A. Agarose gel electrophoresis of hNIS PCR products demonstrated a single band close to 2 K bp. B. Agarose gel electrophoresis of hTPO PCR products demonstrated a single band close to 7.2 K bp.

ered with HEPES, pH 7.3). The cells were then incubated with 3.7 kBq of ^{125}I per well for 0, 5, 10, 20, 40, and 60 min, respectively, in the presence of 0.5 mL of HBSS buffer. After incubation, the medium containing ^{125}I was removed. The cells were then washed twice with ice-cold HBSS buffer and harvested with 100% ice-cold dehydrated alcohol. Cell lysates were collected and measured in a gamma counter (Xi'an Zhida Inc., China). Cell uptake data was presented as counts of radioactivity. Experiments were performed twice with triplicate wells.

The effect of ^{125}I retention was evaluated by the ^{125}I efflux kinetics in PC-3 cells co-expressed with hNIS and hTPO. Briefly, PC-3 cells transfected with Ad-CMV-hTPO, Ad-CMV-hNIS, Ad-CMV-hTPO-2A-hNIS, and control virus were washed twice with HBSS, then incubated with 3.7 kBq of ^{125}I per well at 37°C for 60 min. After washing twice with ice-cold HBSS, cells were incubated in fresh HBSS buffer for additional 5, 15, 30, and 60 min. After incubation, the buffer was removed immediately and cells were harvested with 1 mL of dehydrated alcohol. Cell lysates were collected and measured in a gamma counter (Xi'an Zhida Inc., China). Cell uptake data was presented as counts of radioactivity. Experiments were performed twice with triplicate wells.

Statistical analysis

All experiments were carried out in triplicates unless otherwise indicated. Quantitative data were expressed as mean ± SD. Means were compared using one-way ANOVA and student's t-test. P values of <0.05 were considered statistically significant.

Results

Construction of pAV.Ex1d-CMV>hNIS and pAV.Ex1d-CMV>hTPO/T2A/hNIS by gateway technology

The hNIS and hTPO cDNA genes were successfully obtained as determined by 1) AGE after restriction enzyme digestion, and 2) DNA sequencing map (**Figure 3**). AGE of hNIS after PCR amplification showed a single band around 2 K base pairs (bp) (**Figure 3A**), which is close to the desired size of hNIS (1,932 bp). Further DNA sequencing of hNIS by DNAssit 2.0 software (Changsha Yingrun Biotechnology Co., China) alignment demonstrated that the full length hNIS gene completely matches the DNA sequence of hNIS in the GenBank (ID of hNIS: HH762189.1). The results of AGE and the sequencing map suggested that we successfully obtained the hNIS cDNA gene. In addition, AGE of the hTPO PCR products after EcoRI enzyme digestion showed a single band at the position of 7.2 K bp (**Figure 3B**), locating at the exact size (7.2 K bp) of pDNR-LIB-hTPO-M. DNA sequencing of hTPO PCR products by DNAssit 2.0 software alignment revealed that the full length hTPO gene matched the sequence of hTPO in the GenBank (ID of hTPO: BC095448.1). Combining the results of AGE and DNA sequencing map, we ensured that the construction of hTPO cDNA gene was accomplished as well.

After obtaining the hNIS and hTPO cDNA genes, we constructed the attB1/hNIS/attB2 and attB1/hTPO/T2A/hNIS/attB2 genes using Gateway technology. The primers employed in the PCR amplification of the attB1/hNIS/attB2 and attB1/hTPO/T2A/hNIS/attB2 genes were summarized in **Table 1**. In addition to hNIS sequence, each PCR primer was designed to generate a Gateway-compatible attB1 (forward primer) or attB2 (reverse primer) recombination site flanking the amplified hNIS or hTPO as described previously [18, 19]. Kozak (5'-ACCATG-3') consensus sequences were incorporated into the forward primers to enable that the ATG in the Kozak sequence is in frame with the attB1 site, which allowed terminal fusion proteins to be produced from destination vectors that contain *N*-terminal tags. For fusion of attB1-hTPO-T2A and attB2-hNIS-T2A,

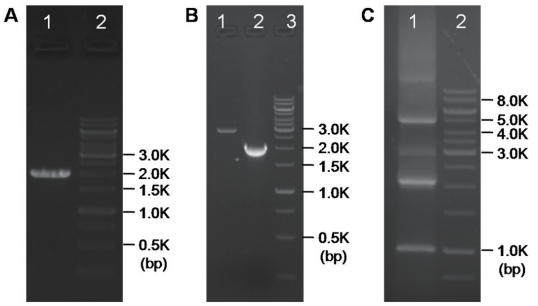

Figure 4. Characterization of attB1/hNIS/attB2 and attB1/hTPO/T2A/hNIS/attB2 by agarose gel electrophoresis. A. A single 2.0 K-band (Lane 1) confirmed the size of attB1/hNIS/attB2. B. Positive bands around 2.8 K bp (Lane 1) and 2.0 K bp (Lane 2) confirmed the sizes of attB1-hTPO/T2A and attB2-hNIS/T2A, respectively. C. A single 4.8 K-band (Lane 1) confirmed the size of attB1-hTPO/T2A/hNIS.

additional complementary primers between hTPO-T2A and T2A-hNIS were designed to generate a full length of attB1/hTPO/T2A/hNIS/attB2. The fusion primer F and fusion primer R (**Table 1**) were introduced to amplify attB1/hTPO/T2A/hNIS/attB2. AGE of the PCR products was performed to verify the fused attB1/hNIS/attB2 and attB1/hTPO/T2A/hNIS/attB2 (**Figure 4**). A single band at the position of 2 K bp in Lane 1 (**Figure 4A**) was clearly identified for attB1-hNIS-attB2, which matched the desired size of 1.9–2 K bp. In addition, as shown in **Figure 4B**, a single band in Lane 1 was determined at the position of 2.8 K bp, which agreed with the desired size of attB1-TPO/T2A (2.6–2.8 K bp); while a single band with 2 K bp was shown in Lane 2, which was consistent with the desired size of attB2-hNIS/T2A (2 K bp). Finally, the AGE of attB1-hTPO/T2A/hNIS PCR products was depicted in Lane 1 (**Figure 4C**). A positive 4.8 K-band was clearly visible, which should be contributed from attB1-hTPO/T2A/hNIS (desired size of 4.6–4.8 K bp). Taken together, the AGE confirmed that 1) attB1 and attB2 were flanked to hNIS and hTPO gene, and 2) attB1/hNIS/attB2 and attB1/hTPO/T2A/hNIS/attB2 were successfully generated by Gateway technology.

In the next step, the amplified attB1/hNIS/attB2 and attB1/hTPO-T2A-hNIS/attB2 were inserted into the vector pDONR™/221 by using the BP Clonase™ II Enzyme Mix. Products from the BP reaction were directly transformed into One Shot stb13 Chemically Competent Cells *E. coli* bacteria. The AGE after restriction enzyme digestion and DNA sequencing map were utilized to characterize the pDown-hNIS and pDown-hTPO/T2A/hNIS genes. AGE of pDown-hNIS was shown in **Figure 5A**. The clear 2.2K-bands in Lane 3–6, and 9 agreed with the desired size of pDown-hNIS (2.1–2.3 K bp). The positive clones shown in Lane 3, 5, and 9 (**Figure 5A**) were selected for DNA sequencing. As shown in **Figure 5B**, the DNA sequence of pDown-hNIS perfectly matched the hNIS DNA sequence in the Genbank (ID of hNIS: HH762189.1) and the sequence of vector pDONR™/221, suggesting pDown-hNIS was successfully constructed. In addition, AGE of pDown-hTPO/T2A/hNIS after EcoRV and XhoI enzyme digestions was performed to verify the correct clone (bands at the positions of ~ 2.6 K and ~ 4.6 K bp). As shown in Lane 1 (**Figure 5C**), positive bands with 2.6 K and 4.7 K bp were obtained. DNA sequence analysis of this clone further confirmed the DNA sequence of pDown-hTPO/T2A/hNIS exactly matched the sequences of hNIS (ID of hNIS: HH762189.1) and hTPO in the GenBank (ID of hTPO: BC095448.1) (**Figure 5D**).

To build up pAV.Ex1d-CMV>hNIS, pAV.Ex1d-CMV>hTPO, and pAV.Ex1d-CMV>hTPO/T2A/hNIS, the obtained pDown-hNIS (or pDown-hTPO; or pDown-hTPO/T2A/hNIS) was inserted into pAV.Des1d destination vectors by an LR reaction. AGE of pAV.Ex1d-CMV>hNIS colony PCR products demonstrated positive destination segment with the size of 2.1 K bp (expected >2 K bp) in all clones as depicted in Lane 1–7 (**Figure 6A**). The clone shown in Lane 2 (**Figure 6A**) was selected for DNA sequence analysis. The result revealed that the DNA sequence of pAV.Ex1d-CMV>hNIS is completely consistent with the hNIS sequence in the Genbank (ID of hNIS: HH762189.1) and sequence of vector pAV.Ex1d-CMV (**Figure 6B**). In addition, both of AGE and sequence analysis were carried out to verify the accomplishment of pAV.Ex1d-CMV>hTPO construction (data not shown). Furthermore, AGE of bacteria colon products after NdeI and BstBI enzyme digestion showed positive 4.7 K-bands in Lane 2, 4, 6, 8, and 10 (**Figure 6C**), which matched the desired size of 4.7 K bp. The AGE results of plasmid (positive control) were shown in Lane 1, 3, 5, 7, and 9 (**Figure 6C**). The clone shown in Lane 4 (**Figure 6C**) was selected for DNA

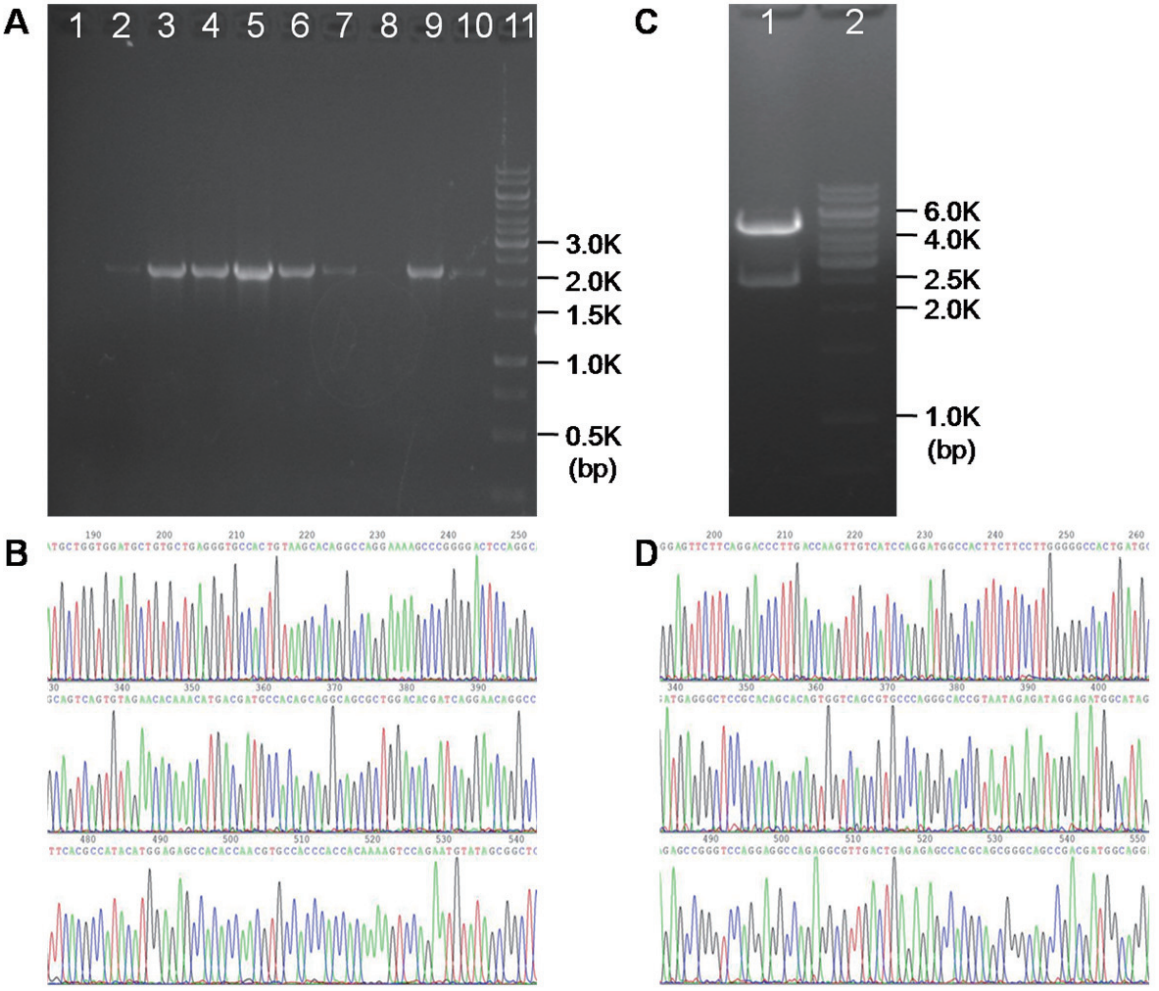

Figure 5. Characterization of pDown-hNIS and pDown-hTPO/T2A/hNIS. A. Agarose gel electrophoresis of pDown-hNIS PCR colony. A desired band with 2.2 K bp was shown in Lane 1–9. B. DNA sequence alignment of pDown-hNIS was found to be consistent with the hNIS sequence in the GenBank. C. Characterization of pDown-hTPO/T2A/hNIS after EcoRV and XhoI enzyme digestion. Positive bands with 2.6 K and 4.7 K bp were obtained which agreed with the desired bands at the positions of ~ 2.6 K and ~ 4.6 K bp. D. DNA sequence alignment of pDown-hTPO/T2A/hNIS was found to be consistent with the hTPO sequence in the GenBank.

sequence analysis. The result demonstrated that the DNA sequence of pAV.Ex1d-CMV>hTPO/T2A/hNIS agreed with the hTPO sequence in the GenBank (ID of hTPO: BC095448.1) and sequence of vector pAV.Ex1d-CMV (**Figure 6D**).

After HEK293 cells were transfected with virus containing hNIS or hTPO-T2A-hNIS genes for 7 days, CPE phenomenon was observed in both cases (**Figure 7A-C**), but not in non-transfected cells (**Figure 7D**), suggesting the viral transfection in cells with the desired gene was achieved. After amplification of HEK293 cells, the amount of virus was titrated using $TCID_{50}$ assay. The titer was determined to be 1×10^{10} PFU/mL for pAV.Ex1d-CMV>hNIS, and 7.94×10^{9} PFU/mL for pAV.Ex1d-CMV>hTPO/T2A/hNIS, respectively.

Double-label immunofluorescence staining of hNIS and hTPO expression in PC-3 cells

Expression of the hNIS and/or hTPO protein in PC-3 cells transfected with pAV.Ex1d-CMV>hTPO/T2A/hNIS or pAV.Ex1d-CMV>hNIS was determined by double-label immunofluorescence staining. As shown in **Figure 8A** and **8B**, the hNIS and hTPO proteins were co-localized on the cell membrane of pAV.Ex1d-CMV>hTPO/T2A/hNIS transfected PC-3 cells,

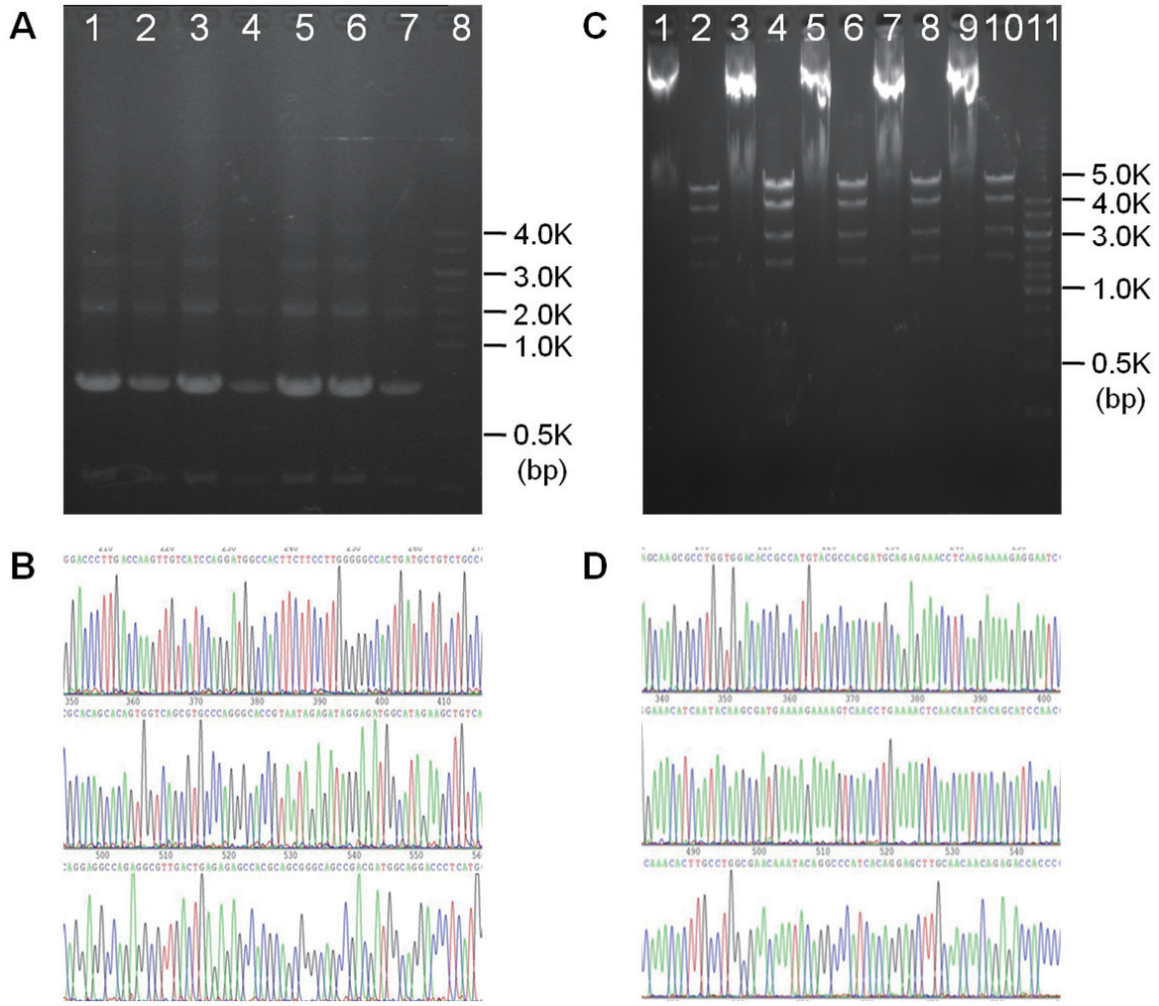

Figure 6. Characterization of pAV.Ex1d-CMV>hNIS and pAV.Ex1d-CMV>hTPO/T2A/hNIS. A. Agarose gel electrophoresis of pAV.Ex1d-CMV>hNIS PCR colony. A desired band with 2.2 K bp was shown in Lane 1–7. B. DNA sequence alignment of pDown-hNIS was found to be consistent with the hNIS sequence in the GenBank. C. Characterization of pAV.Ex1d-CMV>hNIS after NdeI and BstBI enzyme digestion. A 4.7 K-band was observed which agreed with the desired size of 4.7 K bp. D. DNA sequence alignment of pAV.Ex1d-CMV>hTPO/T2A/hNIS was found to be consistent with the hTPO sequence in the GenBank.

suggesting that the positive stainings were attributed to the co-expression of hNIS (green color) and hTPO (red color) protein. Without surprising, the positive staining of hNIS (green color) protein was only observed in the pAV.Ex1d-CMV>hNIS transfected PC-3 cells (**Figure 8C**). There were no positive stainings of hNIS and/or hTPO protein obtained in the non-transfected PC-3 cells (**Figure 8D** and **8E**).

Radioiodine (^{125}I) uptake and retention

Cellular uptake and retention of radioiodine (^{125}I) were examined in PC-3 cells transfected with 1) hNIS and hTPO genes, 2) hNIS gene only, and 3) hTPO gene only. The non-transfected PC-3 cells served as a control group. For cell uptake study, significant enhancement of radioiodine (^{125}I) uptake was observed at all time points (5, 10, 20, 40, 60 min post-incubation of ^{125}I) examined in hNIS-hTPO transfected, and hNIS transfected PC-3 cells as compared to the non-transfected PC-3 cells; whereas for the hTPO-transfected PC-3 cells, no significant enhancement of radioiodine (^{125}I) uptake was observed (**Figure 9A**). Radioiodine (^{125}I) uptake in hNIS-hTPO transfected, and hNIS transfected PC-3 cells rapidly reached the maximum after a short incubation period (5 min) with the uptake ratios of 2.91 ± 0.16 (hNIS-hTPO trans-

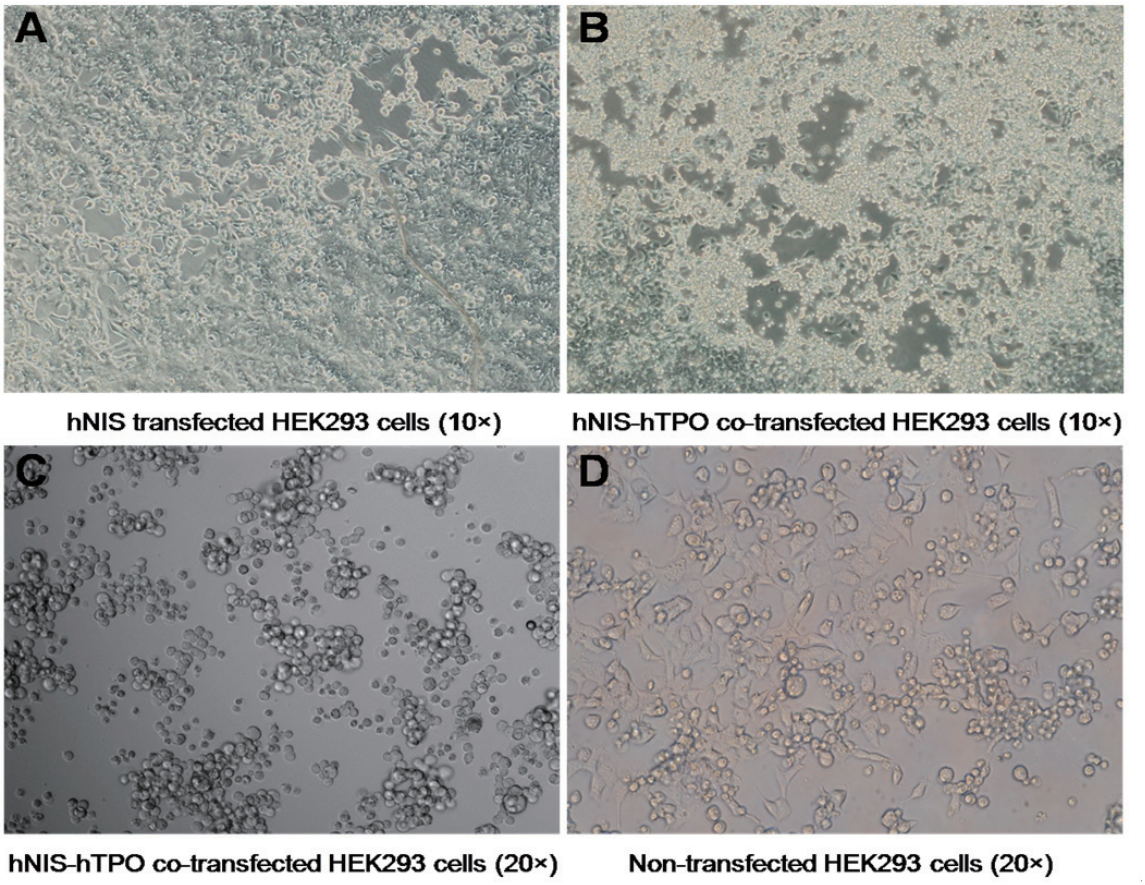

Figure 7. Packaging of integrated Ad5 virus. CPE phenomena were observed in the transfected HEK293 cells (A. pAV.Ex1d-CMV>hNIS; B and C. pAV.Ex1d-CMV>hTPO/T2A/hNIS); but not observed in the non-transfected HEK293 cells (D). 1×10^4 HEK293 cells/well; magnification 10× in A and B; magnification 20× in C and D.

fected group), and 3.81 ± 0.15 (hNIS transfected group), as compared to non-transfected group. During the first hour of incubation, radioiodine (^{125}I) uptake in hNIS-hTPO transfected PC-3 cells (**Figure 9A**, solid line) retained steadily as a function of incubation time, whereas remarkably decreased uptake was observed for the hNIS transfected group (**Figure 9A**, dashed line). After 1 h incubation, as compared to non-transfected group, the uptake ratios of 6.58 ± 0.56 and 3.81 ± 0.15 were determined for the hNIS-hTPO transfected group, and the hNIS transfected group, respectively. In addition, excellent cell retention of radioiodine (^{125}I) was detected in the hNIS-hTPO transfected group, whereas rapid release of ^{125}I was observed in the hNIS transfected group (**Figure 9B**). After 1 h cell efflux study, significant radioiodine (^{125}I) remained in the hNIS-hTPO transfected group with a high ^{125}I retention ratio of 5.47 ± 0.36 as compared to the non-transfected group. For the PC-3 cells transfected with hNIS only or hTPO only, radioiodine (^{125}I) almost completely eluted out from the cells after 1 h cell efflux study.

Discussion

Since the hNIS gene was first cloned [20], hNIS gene transfer for nonthyroidal tumor imaging and therapy has been studied in various cancers, including lung cancer, liver cancer, colon cancer, prostate cancer, and many others [11, 21-28]. In most of these studies, single hNIS gene was usually transferred with a viral or non-viral vector, and different iodine uptake index was determined as compared to non-transferred group. Although the improved iodine uptake was observed in hNIS-transfected group, significant therapeutic effect was hardly to achieve in general, presumably due to the rapid efflux of radioiodine in the tumor, causing

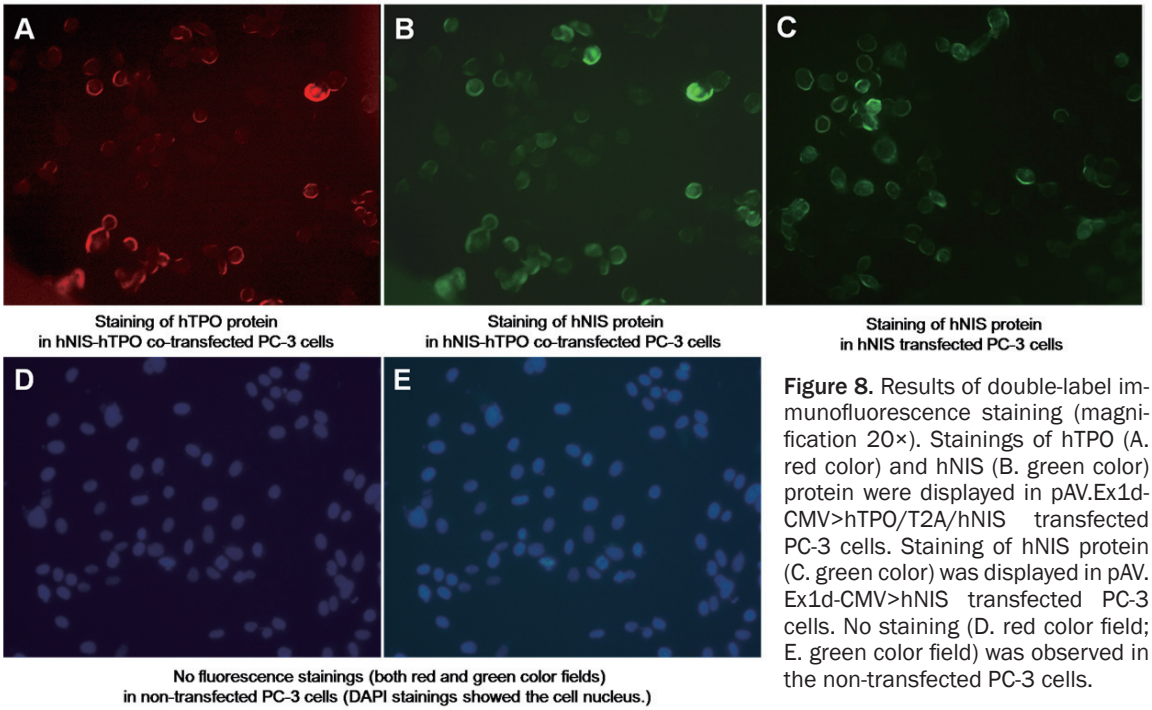

Figure 8. Results of double-label immunofluorescence staining (magnification 20×). Stainings of hTPO (A. red color) and hNIS (B. green color) protein were displayed in pAV.Ex1d-CMV>hTPO/T2A/hNIS transfected PC-3 cells. Staining of hNIS protein (C. green color) was displayed in pAV.Ex1d-CMV>hNIS transfected PC-3 cells. No staining (D. red color field; E. green color field) was observed in the non-transfected PC-3 cells.

minimal retention of radiation dosimetry not enough to affect tumor cell viability [12, 17]. In order to improve the radioiodine retention in non-thyroid tumors, a co-transfection strategy using two plasmid vectors containing either hTPO or hNIS gene was introduced to enhance therapeutic efficiency of radioiodine [12]. However, the experimental data demonstrated that the radioiodine retention was not dramatically enhanced. One possible explanation is that the expression of hTPO and hNIS may be limited due to the low transfection efficacies of multiple plasmid vectors. Co-transfection of the hNIS and hTPO genes by different plasmid vectors may not be an ideal approach, which remains a big challenge to warrant that multiple plasmid vectors can be effectively transfected into the cells afterwards with good ratios and amounts. Consequently, construction of hNIS and hTPO in a multicistronic vector is of great interest as an advanced approach to prolong the radioiodine retention after co-transfection of hNIS and hTPO genes into the tumor cells.

To ascertain the construction of hNIS and hTPO genes in a multicistronic vector, we chose the recombination cloning technology, which circumvents traditional restriction enzyme based cloning limitations, enabling virtual access to any expression system (http://www.invitrogen.com/) [15]. Up to date, highly efficient site-specific recombination-based systems are commercially available, including the Gateway cloning system, which can be used as a general tool of constructing large open reading frame (ORF) clone collections. In addition, the 2A peptide [29-33], or 2A-like sequence, was selected in our study to construct hNIS and hTPO genes in a multicistronic vector. The 2A peptide impairs normal peptide bond formation between the 2A glycine and the 2B proline without affecting the translation of 2B [29]. The utility of the 2A peptide allows the stoichiometric production of up to four proteins from a single vector through a ribosomal skip mechanism [33]. By using Gateway technology and 2A method, we attempted to recombine full-length hNIS and hTPO genes into a single Ad5 viral vector. However, the hNIS gene contains 1,932 bp while the hTPO gene includes 2,802 bp; both are considered as the genes with large size. Recombination of two large genes into one viral vector could be problematic in terms of gene combination techniques. Actually, in our first attempt at performing PCR amplification of attB1/hTPO/T2A/hNIS/attB2, the yield of product was relatively low as compared to that in the usual case using the Gateway approach. One pair of primers (Fusion primer F and R) was

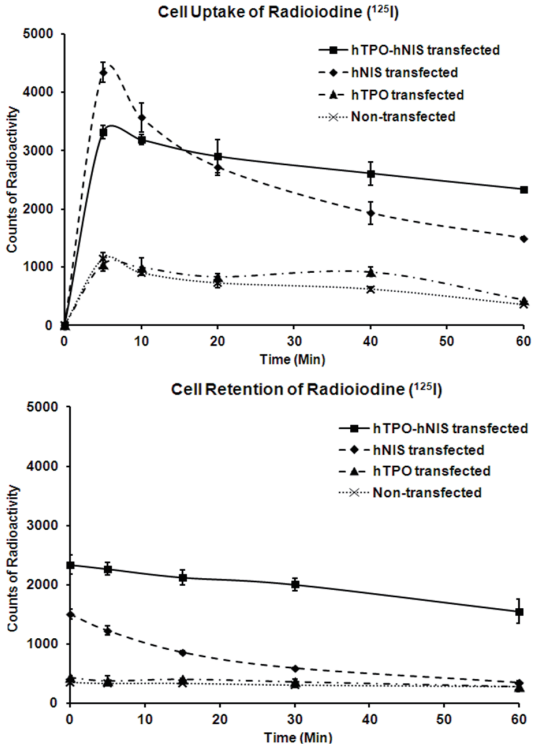

Figure 9. Time course of hTPO-hNIS-, hNIS-, and hTPO- mediated radioiodine (^{125}I) uptake (A) and retention (B) in transfected PC-3 cells as compared to non-transfected.

thus incorporated to improve the product yield. As detailed in the section 3.1, hNIS and hTPO genes were successfully constructed in a multicistronic vector confirmed by systematical characterizations. The obtained vector was then transfected into HEK293 cells. The titration of the recombinant adenoviral vector carrying hTPO-T2A-hNIS was determined to be 7.94 × 10^9 PFU/mL by using the TCID50 assay, suggesting the vector transfection was quite efficient.

To further prove our concept, PC-3 prostate cancer cell line was selected for the immunofluorescence staining, and radioiodine uptake and efflux studies. Prostate cancer is the most common cancer and the second leading cause of cancer-related deaths in men in the US [34, 35]. The traditional therapeutic options for patients with prostate cancer include radical prostatectomy, treatment with cytotoxic chemotherapeutic agents, radiotherapy and hormone therapy. Although prognosis of prostate cancer is generally excellent, androgen-independent prostate cancer is associated with poor prognosis and new treatment modalities are therefore urgently needed [36, 37]. In recent years, numerous researches [38-41] about genetic therapies in prostate cancer have provided promising approaches for the treatment of this neoplasm including single hNIS transgene. In addition, prostate cancer is usually close to body surface and relatively easier for injection of gene therapy vehicles, such as adenoviral vector, making the translation of *in vitro* findings to *in vivo* studies less challenging. As a result, PC-3 cell line derived from advanced androgen-independent bone metastasized prostate cancer was chosen as our study subject. As shown in **Figure 8A** and **8B**, the immunofluoresence staining demonstrated that the hNIS and hTPO proteins were co-localized on the cell membrane of PC-3 cells after pAV.Ex1d-CMV>hTPO/T2A/hNIS transfection, suggesting that hNIS and hTPO proteins were truly co-expressed in the transfected PC-3 cells as we expected. For the cell uptake study, the overall higher uptake of radioiodine (^{125}I) was observed in the hNIS-hTPO transfected group as compared to the hNIS-, or hTPO-transfected group, and non-transfected group. However, at the early time points (<15 min), uptake values in the hNIS-hTPO transfected group were slightly lower than those in the hNIS-transfected group. One possible explanation is that the hNIS protein expression in the hNIS-transfected group may be slightly higher than that in the hNIS-hTPO transfected group, considering the large size effect of recombination of both hNIS and hTPO genes into a single vector. For the cell retention study, better radioiodine (^{125}I) retention in the hNIS-hTPO transfected group was observed at all time points (5, 15, 30, and 60 min) examined as compared to the hNIS-, or hTPO-transfected group, and non-transfected group (**Figure 9**), indicating that the improved radioiodine retention was indeed contributed from the hTPO-mediated organification. Overall, the multicistronic co-expression of hTPO and hNIS genes in PC-3 cells led to a synergistic effect for the improved radioiodine uptake and retention.

It is worthy to note that cytomegalovirus (CMV) promoter, one of the most commonly used promoters for expression of transgenes in mammalian cells, was used in our study. Although prostate cancer PC-3 cell line was selected for

this proof-of-concept study, our newly constructed vector has the potential to be applied to other tumor cell lines. More broadly, after replacing the CMV promoter with other tumor or tissue specific promoters, such as PEG3 (progression elevated gene-3) or survivin, the resulting multicistronic genes may promote even better tumor specificity, leading to more favorable properties in terms of radioiodine uptake and retention. Further modifications of multicistronic vector and translation of our *in vitro* findings to *in vivo* studies are currently underway.

Conclusion

We successfully constructed a single Ad5 viral vector by introducing the T2A between hNIS and hTPO genes with Gateway cloning system. It is the first time to combine two large size genes (hNIS and hTPO) in a single Ad5 adenoviral vector. Our results from the radioiodine (^{125}I) uptake and retention studies demonstrated that the hTPO mediated by hNIS can enhance the uptake (after 1 h incubation time) and retention of radioiodine in transfected prostate cancer PC-3 cells as compared to the single gene-transfected and non-transfected groups. We anticipate that this advanced approach will provide valuable information for better understanding and improving hNIS-hTPO mediated radioiodine gene therapy.

Acknowledgments

The authors are grateful for the support of the National Natural Science Foundation of China (Grant No. 30800275, 30970846, and 30970847), the Major Program of National Natural Science Foundation of China (Grant No. 81230276 and 81090270), and the USC Molecular Imaging Center.

Abbreviations

hNIS, human sodium/iodide symporter; hTPO, human thyroperoxidase; CMV, cytomegalovirus; T2A, Thosea asigna virus 2A sequence; Ad5, adenovirus serotype 5; CPE, cytopathic effects; MOI, multiplicity of infection; bp, base pair; AGE, agarose gel electrophoresis; PBS, phosphate buffered saline; HBSS, Hank's buffered salt solution; PCR, polymerase chain reaction; BSA, bovine serum albumin.

Address correspondence to: Dr. Jing Wang, Department of Nuclear Medicine, Xijing Hospital, The Fourth Military Medical University, Xi'an, Shaanxi, China, 710032. Tel: +86 029 84775449; Fax: +86 029 81230242; E-mail: wangjing@fmmu.edu.cn; Dr. Kai Chen, Molecular Imaging Center, Department of Radiology, Keck School of Medicine, University of Southern California, CA 90033, USA. Tel: +1 323 442 3858; Fax: +1 323 442 3253; E-mail: chenkai@usc.edu.

References

[1] Nilsson M. Molecular and cellular mechanisms of transepithelial iodide transport in the thyroid. Biofactors 1999; 10: 277-85.

[2] Trapasso F, Iuliano R, Chiefari E, Arturi F, Stella A, Filetti S, Fusco A, Russo D. Iodide symporter gene expression in normal and transformed rat thyroid cells. Eur J Endocrinol 1999; 140: 447-51.

[3] Filetti S, Bidart JM, Arturi F, Caillou B, Russo D, and Schlumberger M. Sodium/iodide symporter: a key transport system in thyroid cancer cell metabolism. Eur J Endocrinol 1999; 141: 443-57.

[4] Lazar V, Bidart JM, Caillou B, Mahe C, Lacroix L, Filetti S, Schlumberger M. Expression of the Na+/I- symporter gene in human thyroid tumors: a comparison study with other thyroid-specific genes. J Clin Endocrinol Metab 1999; 84: 3228-34.

[5] Reiners C and Farahati J. 131I therapy of thyroid cancer patients. Q J Nucl Med 1999; 43: 324-35.

[6] Uyttersprot N, Pelgrims N, Carrasco N, Gervy C, Maenhaut C, Dumont JE, Miot F. Moderate doses of iodide in vivo inhibit cell proliferation and the expression of thyroperoxidase and Na+/I- symporter mRNAs in dog thyroid. Mol Cell Endocrinol 1997; 131: 195-203.

[7] Ahn SJ, Jeon YH, Lee YJ, Lee YL, Lee SW, Ahn BC, Ha JH, Lee J. Enhanced anti-tumor effects of combined MDR1 RNA interference and human sodium/iodide symporter (NIS) radioiodine gene therapy using an adenoviral system in a colon cancer model. Cancer Gene Ther 2010; 17: 492-500.

[8] Ma XJ, Huang R, and Kuang AR. AFP promoter enhancer increased specific expression of the human sodium iodide symporter (hNIS) for targeted radioiodine therapy of hepatocellular carcinoma. Cancer Invest 2009; 27: 673-81.

[9] Guo R, Zhang Y, Liang S, Xu H, Zhang M, and Li B. Sodium butyrate enhances the expression of baculovirus-mediated sodium/iodide sym-

porter gene in A549 lung adenocarcinoma cells. Nucl Med Commun 2010; 31: 916-21.

[10] Barton KN, Stricker H, Elshaikh MA, Pegg J, Cheng J, Zhang Y, Karvelis KC, Lu M, Movsas B, Freytag SO. Feasibility of adenovirus-mediated hNIS gene transfer and 131I radioiodine therapy as a definitive treatment for localized prostate cancer. Mol Ther 2011; 19: 1353-9.

[11] Klutz K, Willhauck MJ, Wunderlich N, Zach C, Anton M, Senekowitsch-Schmidtke R, Göke B, Spitzweg C. Sodium iodide symporter (NIS)-mediated radionuclide ((131)I, (188)Re) therapy of liver cancer after transcriptionally targeted intratumoral in vivo NIS gene delivery. Hum Gene Ther 2011; 22: 1403-12.

[12] Huang M, Batra RK, Kogai T, Lin YQ, Hershman JM, Lichtenstein A, Sharma S, Zhu LX, Brent GA, Dubinett SM. Ectopic expression of the thyroperoxidase gene augments radioiodide uptake and retention mediated by the sodium iodide symporter in non-small cell lung cancer. Cancer Gene Ther 2001; 8: 612-8.

[13] Smith LM, Sanders JZ, Kaiser RJ, Hughes P, Dodd C, Connell CR, Heiner C, Kent SB, Hood LE. Fluorescence detection in automated DNA sequence analysis. Nature 1986; 321 :674-9.

[14] Tamary H, Surrey S, Kirschmann H, Shalmon L, Zaizov R, Schwartz E, Rappaport EF. Systematic use of automated fluorescence-based sequence analysis of amplified genomic DNA for rapid detection of point mutations. Am J Hematol 1994; 46: 127-33.

[15] Grigorov B, Rabilloud J, Lawrence P, and Gerlier D. Rapid titration of measles and other viruses: optimization with determination of replication cycle length. PLoS One 2011; 6: e24135.

[16] Vaidya SR, Brown DW, Jin L, Samuel D, Andrews N, and Brown KE. Development of a focus reduction neutralization test (FRNT) for detection of mumps virus neutralizing antibodies. J Virol Methods 2010; 163: 153-6.

[17] Weiss SJ, Philp NJ, and Grollman EF. Iodide transport in a continuous line of cultured cells from rat thyroid. Endocrinology 1984; 114: 1090-8.

[18] Hartley JL, Temple GF, and Brasch MA. DNA cloning using in vitro site-specific recombination. Genome Res 2000; 10: 1788-95.

[19] Brandner CJ, Maier RH, Henderson DS, Hintner H, Bauer JW, and Onder K. The ORFeome of Staphylococcus aureus v 1.1. BMC Genomics 2008; 9: 321.

[20] Dai G, Levy O, and Carrasco N. Cloning and characterization of the thyroid iodide transporter. Nature 1996; 379: 458-60.

[21] Yin HY, Zhou X, Wu HF, Li B, and Zhang YF. Baculovirus vector-mediated transfer of NIS gene into colon tumor cells for radionuclide therapy. World J Gastroenterol 2010; 16: 5367-74.

[22] Huang R, Ma X, Li S, Mu D, Gong R, and Kuang A. Radioiodide treatment mediated by adenovirus transfer of human sodium iodide symporter gene into androgen-independent prostate cancer. Sheng Wu Yi Xue Gong Cheng Xue Za Zhi 2010; 27: 1080-4.

[23] Klutz K, Russ V, Willhauck MJ, Wunderlich N, Zach C, Gildehaus FJ, Göke B, Wagner E, Ogris M, Spitzweg C. Targeted radioiodine therapy of neuroblastoma tumors following systemic nonviral delivery of the sodium iodide symporter gene. Clin Cancer Res 2009; 15: 6079-86.

[24] Rao VP, Miyagi N, Ricci D, Carlson SK, Morris JC 3rd, Federspiel MJ, Bailey KR, Russell SJ, McGregor CG. Sodium iodide symporter (hNIS) permits molecular imaging of gene transduction in cardiac transplantation. Transplantation 2007; 84: 1662-6.

[25] Kim KI, Kang JH, Chung JK, Lee YJ, Jeong JM, Lee DS, Lee MC. Doxorubicin enhances the expression of transgene under control of the CMV promoter in anaplastic thyroid carcinoma cells. J Nucl Med 2007; 48: 1553-61.

[26] Niu G, Krager KJ, Graham MM, Hichwa RD, and Domann FE. Noninvasive radiological imaging of pulmonary gene transfer and expression using the human sodium iodide symporter. Eur J Nucl Med Mol Imaging 2005; 32: 534-40.

[27] Dwyer RM, Bergert ER, O'Connor M K, Gendler SJ, and Morris JC. In vivo radioiodide imaging and treatment of breast cancer xenografts after MUC1-driven expression of the sodium iodide symporter. Clin Cancer Res 2005; 11: 1483-9.

[28] Cengic N, Baker CH, Schutz M, Goke B, Morris JC, and Spitzweg C. A novel therapeutic strategy for medullary thyroid cancer based on radioiodine therapy following tissue-specific sodium iodide symporter gene expression. J Clin Endocrinol Metab 2005; 90: 4457-64.

[29] Donnelly ML, Luke G, Mehrotra A, Li X, Hughes LE, Gani D, Ryan MD. Analysis of the aphthovirus 2A/2B polyprotein 'cleavage' mechanism indicates not a proteolytic reaction, but a novel translational effect: a putative ribosomal 'skip'. J Gen Virol 2001; 82: 1013-25.

[30] de Felipe P. Polycistronic viral vectors. Curr Gene Ther 2002; 2: 355-78.

[31] de Felipe P. Skipping the co-expression problem: the new 2A "CHYSEL" technology. Genet Vaccines Ther 2004; 2: 13.

[32] Ryan MD and Drew J. Foot-and-mouth disease virus 2A oligopeptide mediated cleavage of an artificial polyprotein. EMBO J 1994; 13: 928-33.

[33] Szymczak AL, Workman CJ, Wang Y, Vignali KM, Dilioglou S, Vanin EF, Vignali DA. Correc-

tion of multi-gene deficiency in vivo using a single 'self-cleaving' 2A peptide-based retroviral vector. Nat Biotechnol 2004; 22: 589-94.
[34] Damber JE and Aus G. Prostate cancer. Lancet 2008; 371: 1710-21.
[35] Jani AB, Johnstone PA, Liauw SL, Master VA, and Rossi PJ. Prostate cancer modality time trend analyses from 1973 to 2004: a Surveillance, Epidemiology, and End Results registry analysis. Am J Clin Oncol 2010; 33: 168-72.
[36] Di Lorenzo G and De Placido S. Hormone refractory prostate cancer (HRPC): present and future approaches of therapy. Int J Immunopathol Pharmacol 2006; 19: 11-34.
[37] Sternberg CN. Highlights of contemporary issues in the medical management of prostate cancer. Crit Rev Oncol Hematol 2002; 43: 105-21.
[38] Dash R, Azab B, Shen XN, Sokhi UK, Sarkar S, Su ZZ, Wang XY, Claudio PP, Dent P, Dmitriev IP, Curiel DT, Grant S, Sarkar D, Fisher PB. Developing an effective gene therapy for prostate cancer: New technologies with potential to translate from the laboratory into the clinic. Discov Med 2011; 11: 46-56.
[39] Lu M, Freytag SO, Stricker H, Kim JH, Barton K, and Movsas B. Adaptive seamless design for an efficacy trial of replication-competent adenovirus-mediated suicide gene therapy and radiation in newly-diagnosed prostate cancer (ReCAP Trial). Contemp Clin Trials 2011; 32: 453-60.
[40] Takahashi S, Kato K, Nakamura K, Nakano R, Kubota K, and Hamada H. Neural cell adhesion molecule 2 as a target molecule for prostate and breast cancer gene therapy. Cancer Sci 2011; 102: 808-14.
[41] Vajda A, Marignol L, Foley R, Lynch TH, Lawler M, and Hollywood D. Clinical potential of gene-directed enzyme prodrug therapy to improve radiation therapy in prostate cancer patients. Cancer Treat Rev 2011; 37: 643-54.